



HAL
open science

High Cycle Fatigue strength evaluation of welded joints in handling equipment

Hugo Heyraud, Camille Robert, Charles Mareau, Franck Morel, Daniel Bellett, Nicolas Belhomme, Olivier Dore, Jean-Yves Auge

► **To cite this version:**

Hugo Heyraud, Camille Robert, Charles Mareau, Franck Morel, Daniel Bellett, et al.. High Cycle Fatigue strength evaluation of welded joints in handling equipment. *Procedia Structural Integrity*, 2019, 19, pp.566 - 574. <10.1016/j.prostr.2019.12.061>. <hal-03488480>

HAL Id: hal-03488480

<https://hal.science/hal-03488480v1>

Submitted on 21 Jul 2022

HAL is a multi-disciplinary open access archive for the deposit and dissemination of scientific research documents, whether they are published or not. The documents may come from teaching and research institutions in France or abroad, or from public or private research centers.

L'archive ouverte pluridisciplinaire **HAL**, est destinée au dépôt et à la diffusion de documents scientifiques de niveau recherche, publiés ou non, émanant des établissements d'enseignement et de recherche français ou étrangers, des laboratoires publics ou privés.



Distributed under a Creative Commons CC BY-NC 4.0 - Attribution - Non-commercial use - International License



Fatigue Design 2019

High Cycle Fatigue strength evaluation of welded joints in handling equipment

Hugo Heyraud^{a,b}, Camille Robert^a, Charles Mareau^a, Franck Morel^a, Daniel Bellett^a,
Nicolas Belhomme^b, Olivier Dore^b, Jean-Yves Auge^b

^aLAMPA, Art et Métiers Paristech, 2 Boulevard du Ronceray, 49035 Angers, France

^bManitou Group 44158, Ancenis, France

Abstract

This study falls within the scope of the fatigue design of handling machines manufactured by the Manitou Group, which are usually composed of a chassis and a boom. These welded assemblies are subjected to fatigue loading conditions and include highly stressed zones acting as crack initiation sites. In view of the geometrical complexity of the structures, the degree of conservatism incorporated in design methods based on the usual international standards is difficult to evaluate. Alternative design approaches based on the structural stress are being developed and used by other companies such as PSA and LOHR. The present work focuses on developing a numerical approach to take into account the local stiffness of welds. The proposed strategy is based on shell finite element modelling of the assembly and an equivalent stiffness matrix for welds. This makes it possible to describe the local mechanical behaviour of seam welds with the computational cost of a shell element based model. To validate the proposed approach, a comparison in terms of stiffness is undertaken for three welded structures using solid finite element models as a reference. The proposed approach is also compared to the Manitou, Fayard and Lohr approaches.

© 2019 The Authors. Published by Elsevier B.V.

Peer-review under responsibility of the Fatigue Design 2019 Organizers.

Keywords: Welded Joints; Finite Elements; 2D-3D model;

1. Introduction

Handling equipment manufactured by Manitou is generally composed of two structural sub-assemblies: the chassis and the boom. Both of these geometrically complex welded assemblies are entirely manufactured by Manitou (see figure 4), principally from grade S355 sheet steel assembled by gas metal arc welding. To design the chassis and the boom, finite element calculations are coupled to full-scale tests for different loading conditions. Shell elements are used to model the welded assemblies, in which the local stiffness of the seam welds is not considered. The numerical method currently used is time-efficient but the stiffness behaviour of the welded structures is not well represented. Bennebach [1] identified several methods used in industry for the fatigue design of welded assemblies. Most are based on finite element models using shell elements in which the seam welds are idealised in order to limit the computational cost. The variety of finite element models presented in [1] and in the literature [2], [3], [4] highlights the difficulty in defining a unique methodology to design welded assemblies.

The aim of this work is to develop a fatigue design approach that can be applied to any type of welded joint found on

2210-7843 © 2019 The Authors. Published by Elsevier B.V.

Peer-review under responsibility of the Fatigue Design 2019 Organizers.

© 2019 published by Elsevier. This manuscript is made available under the CC BY NC user license

<https://creativecommons.org/licenses/by-nc/4.0/>

Manitou handling equipment. More exactly, the objective is to propose a finite element model based on shell elements with an equivalent weld stiffness with regard to solid element models as well as the modelled weld detail.

In the first section of this article the model currently used by Manitou is presented. Then, the strategy proposed by [5] and [6] are presented. The model currently used by the PSA Group [5], [7] involves a specific meshing rule and seam welds are represented by rigid connexions between welded steel sheets. The second model, initially proposed by the Volvo car company [8], has been extended by Turlier [6], [9] to weld root fatigue assessment. Seam welds are modelled by an inclined shell element row connected to steel sheets by a combination of 1D rigid elements and MPC. Then, an alternative finite element model is proposed. Shell element are used to model the steel sheets and the seam welds are represented by an equivalent stiffness matrix. To compare the stiffness behaviour of these strategies, 3 welded structures representatives of a Manitou chassis are modelled and the different strategies are compared to a reference solution obtained from solid elements.

Nomenclature

E	the Young modulus
ν	the Poisson ratio's
ϵ_{11}	in plane strains \vec{X}
ϵ_{22}	in plane strains \vec{Y}
ϵ_{33}	out of plane strains \vec{Z}
σ_{11}	in plane stress \vec{X}
σ_{22}	in plane stress \vec{Y}
σ_{33}	out of plane stress \vec{Z}
H^J	interpolated functions at node(J)
MPC	multi-point constraint

2. Different finite element models for welded assemblies

2.1. The Manitou model

The model currently used by Manitou to design welded assemblies is based on CQUAD4 shell elements, implemented in the Nastran software, to model the mid surface of steel sheets. The local stiffness from the seam welds is not taken into account. At steel sheet junctions, shell elements are node-to-node connected as showed in figure 1.

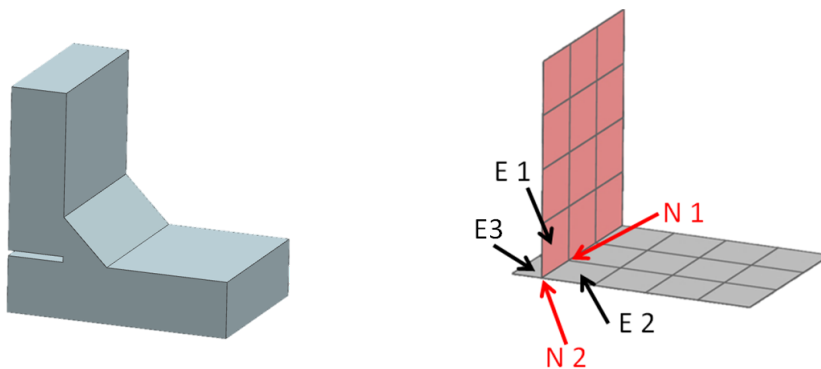


Fig. 1. Finite element model used by Manitou to design welded assemblies. The weld rigidity is not taken into account and the shell elements are node-to-node connected to ensure model consistency. The six degrees of freedom of the nodes N1 and N2 are common for the three elements E1,E2,E3.

2.2. The Fayard model

The PSA Group currently uses the method proposed by Fayard [5] to design welded assemblies. The steel sheets mid surfaces are modelled by CQUAD4 shell element and the local stiffness of the welds is taken into account by a rigid element. The extremity of each 1D rigid element is located at the mid length of the weld leg as shown in figure 2.

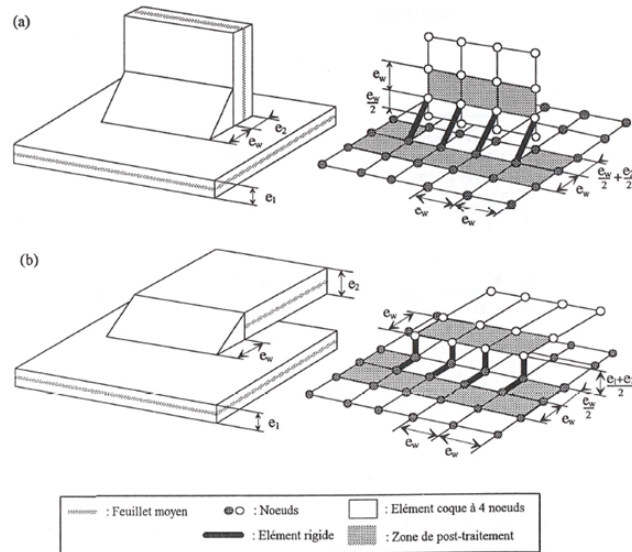


Fig. 2. Finite element model used by PSA to design welded assemblies applied to T-joints (a) and overlap joints (b) [5]

2.3. The Lohr model

To deal with fatigue crack at the weld root, Turlier [6] proposed a finite element model based on shell elements, 1D rigid elements and kinematic connexions. The steel sheet mid-surfaces are modelled by shell elements and the seam welds by slanted shell elements. The thickness of the seam weld shell elements is equal to the weld throat size. The connexion between the slanted shell elements and the steel sheet shell elements is made by rigid elements (RBE2) and MPC as shown in figure 3.

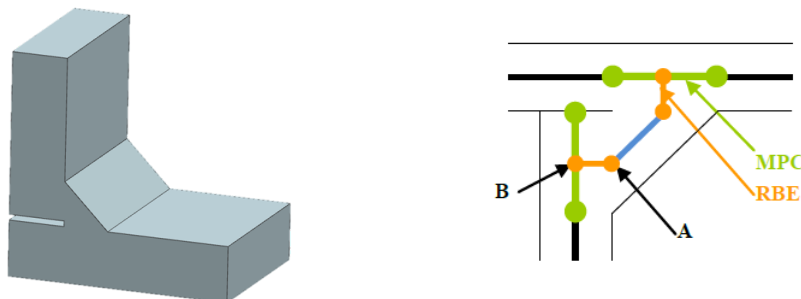


Fig. 3. The Lohr model : Shell element connexion in the weld area. The blue element represents the weld, the orange elements are the 1D rigid element and the MPC are in green. The 1D rigid element is connected to the weld shell element at A and to the MPC at B. The MPC insures the connexion with elements of the steel sheets [6]

3. The proposed model

Manitou chassis are large geometrically complex structures composed of a variety of welded details as shown in figure 4.

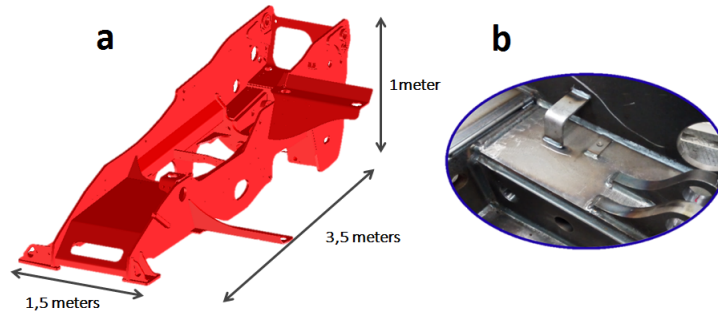


Fig. 4. (a) a Manitou chassis with classical dimensions, (b) typical welded assembly

To improve the modelling currently used by Manitou, the local stiffness of the welds should be considered.

To achieve this, the proposed strategy involves modelling the steel sheets with shell elements and replacing the welds with an equivalent stiffness element, whose stiffness matrix has been estimated a priori. Therefore, the global model includes only shell elements in which the welded areas are taken into account by stiffness terms added on the degree of freedom (DOF) of the shell element nodes closest to the weld areas. Figure 5 shows a L joint modelled with this method.

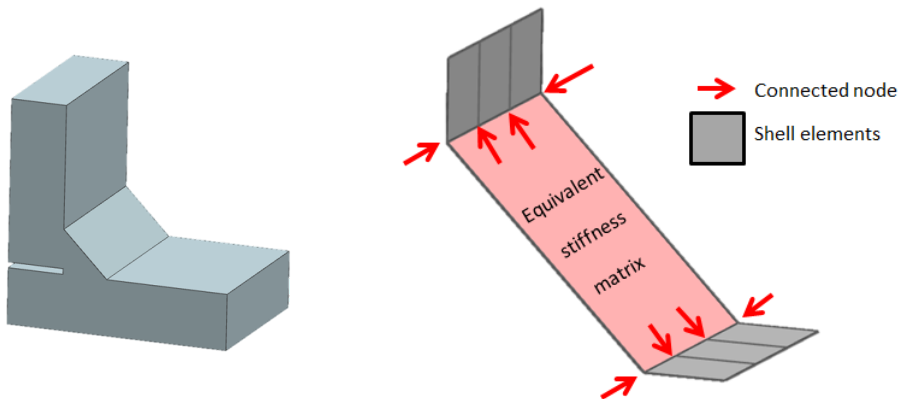


Fig. 5. Equivalent stiffness matrix inserted in the shell element model

To identify the stiffness components of the matrix, the welded areas must be modelled. Solid elements are used to model the welds and the plates under the weld legs. Solid elements are then connected to a row of shell elements. The equivalent matrix results from the condensation of the 2D/3D models on the shell boundary nodes (see Figure 6).

3.1. Shell elements - solid elements connexion

Shell elements and solid elements can not be directly connected due to the non compatibility between the number of DOF of these elements. Fezans [10] proposed relations to express the displacement of a given point in the shell element local coordinate system according to the six DOF of shell element nodes. These relations can be adapted to connect shell and solid elements. To ensure the displacement continuity between the shell and solid elements, the following equations must take into account:

- The three translations at the solid and shell element nodes
- The three rotations at the shell element nodes
- The shell element shape functions

In view of these conditions, the displacement of a solid element node can be expressed as

$$\begin{pmatrix} u_1(I) \\ u_2(I) \\ u_3(I) \end{pmatrix} = \sum_{J=1}^K H^J \begin{pmatrix} U(J) \\ V(J) \\ W(J) \end{pmatrix} + t \sum_{J=1}^K H^J [\phi^J] \begin{pmatrix} \theta_U(J) \\ \theta_V(J) \\ \theta_W(J) \end{pmatrix} \quad (1)$$

where

$\begin{pmatrix} u_1(I) \\ u_2(I) \\ u_3(I) \end{pmatrix}$ is the three DOF of node (I) of the solid element

$\begin{pmatrix} U(J) \\ V(J) \\ W(J) \end{pmatrix}$ is the three translational DOF of node (J) of the shell element

$\begin{pmatrix} N_1 \\ N_2 \\ N_3 \end{pmatrix}$ is the normal vector to the shell element, $[\phi^J] = \begin{bmatrix} 0 & N_3 & -N_2 \\ -N_3 & 0 & N_1 \\ N_2 & -N_1 & 0 \end{bmatrix}$

$t = (I\vec{J}|\vec{N})$, is the shell element thickness

These equations ensure the continuity of the displacement in the in-plane shell element directions. However, in the normal direction, the shell element strains are null (i.e. the Mindlin hypothesis) as well as the Poisson ratio induced displacement by in-plane deformation. At this stage a displacement discontinuity remains between shell and solid elements. To take into account the Poisson ratio induced displacement, an out-of-plane shell element strain must be defined from the in-plane strains. The in-plane strains can be expressed as:

$$\epsilon_{11} = \frac{1}{E}\sigma_{11} - \frac{\nu}{E}\sigma_{22} \quad (2)$$

$$\epsilon_{22} = \frac{1}{E}\sigma_{22} - \frac{\nu}{E}\sigma_{11} \quad (3)$$

And the out-of-plane strain can be expressed as ϵ_{33}

$$\epsilon_{33} = \frac{1}{E}0 - \frac{\nu}{E}(\sigma_{11} + \sigma_{22}) \quad (4)$$

Therefore ϵ_{33} can be expressed as a function of ϵ_{11} and ϵ_{22} as:

$$\epsilon_{33} = \frac{-\nu}{(1-\nu)}(\epsilon_{11} + \epsilon_{22}) \quad (5)$$

From the out-of-plane strain ϵ_{33} , the Poisson ratio induced displacement for a shell element can be written as:

$$D_p(A) = \frac{-\nu}{(1-\nu)}t \left(\frac{(U_2 - U_1)}{D} + H_1 \frac{(V_4 - V_1)}{d} + H_2 \frac{(V_3 - V_2)}{d} \right) \quad (6)$$

where,

U_j : is the Poisson ratio induced displacement in the \vec{X} direction

V_j : is the Poisson ratio induced displacement in the \vec{Y} direction

d, D : is the edge width and length of the shell element

3.2. Identification of the stiffness matrix components

From the 2D-3D model defined in section 3.1 the components of the stiffness matrix can be identified. The principle is to condense the 2D-3D model on the boundary nodes of the shell elements (see figure 6).

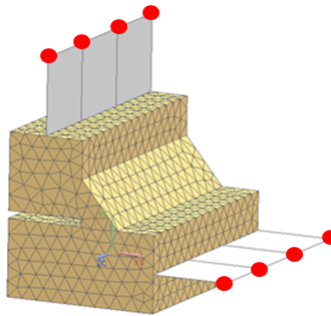


Fig. 6. 2D-3D model. The red dots indicate the boundary nodes of the shell elements

In order to reduce the computational cost, the global stiffness matrix is first factorized (LDLT decomposition), the following system is then solved:

$$K_{factorized}U = F \quad (7)$$

For each step of the identification procedure, a DOF of a boundary node is made equal to unity (1.0) and the others set to zero. After calculation, the reaction forces on the boundary nodes are extracted to build a row of the equivalent stiffness matrix. As the resultant matrix is symmetric only the lower part is stored. For each weld detail, the identification process must be conducted in order to take into account the influence of local geometry on the stiffness behaviour.

4. Stiffness comparison

To validate the stiffness behaviour of the proposed approach, the following three elementary welded structures are considered:

- Structure 1: T joint
- Structure 2: Gusset
- Structure 3: Lap joint

For each geometry, the model is compared to a full "solid elements" model which is considered to be the reference model. The Manitou, Fayard, Lohr approaches are also compared. To compute the reference models, the complete geometries are considered and a refined finite element mesh using 4-node tetrahedral elements(tetra4) is used.

4.1. Geometrical parameters of the elementary welded structures

The three welded structures are made of 8 mm thick steel sheets and the dimension of the weld throat 3.5 millimetres. At the weld root, steels sheets are spaced 1 millimetre from each other. Figure 7 shows the geometrical dimensions of these structures,

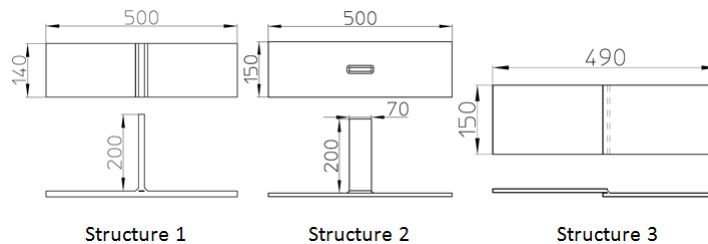


Fig. 7. Geometrical dimensions of structures 1,2,3, in millimetres

4.2. Boundary conditions and loading

For structures 1 and 2, the right and left extremities of the bottom plate are clamped and a load of 1kN is applied at the extremity of the top plate in the three orthogonal directions. For structure 3, the right extremity is clamped and a load of 1kN is applied at the left extremity in the three orthogonal directions. These conditions are summarized in figure 8

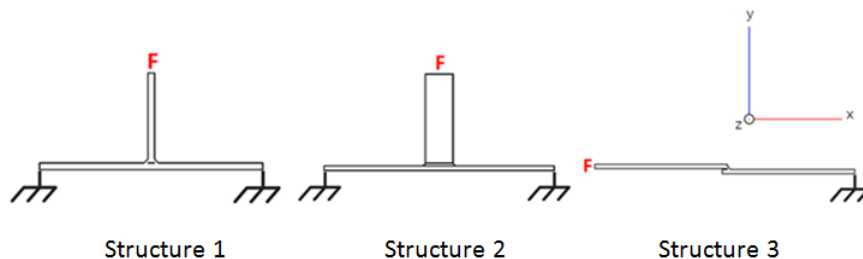


Fig. 8. Boundary conditions and loads applied on structures 1,2,3

4.3. Results

For each welded structure, the stiffness behaviour resulting from the 4 investigated approaches are compared to the reference solid element model. The three reference models have the following DOF:

- Structure 1: 4370145 DOF
- Structure 2: 3973293 DOF
- Structure 3: 4928424 DOF

For each structure, 3 cases are considered corresponding to a load of 1kN in the directions \vec{x} , \vec{y} and \vec{z} . To estimate the stiffness behaviour of each structure, the resulting displacement in the loading direction is averaged over the nodes where the load is applied. The discrepancies between the reference models and the 4 shell based models are presented in figure 9 for each loading case.

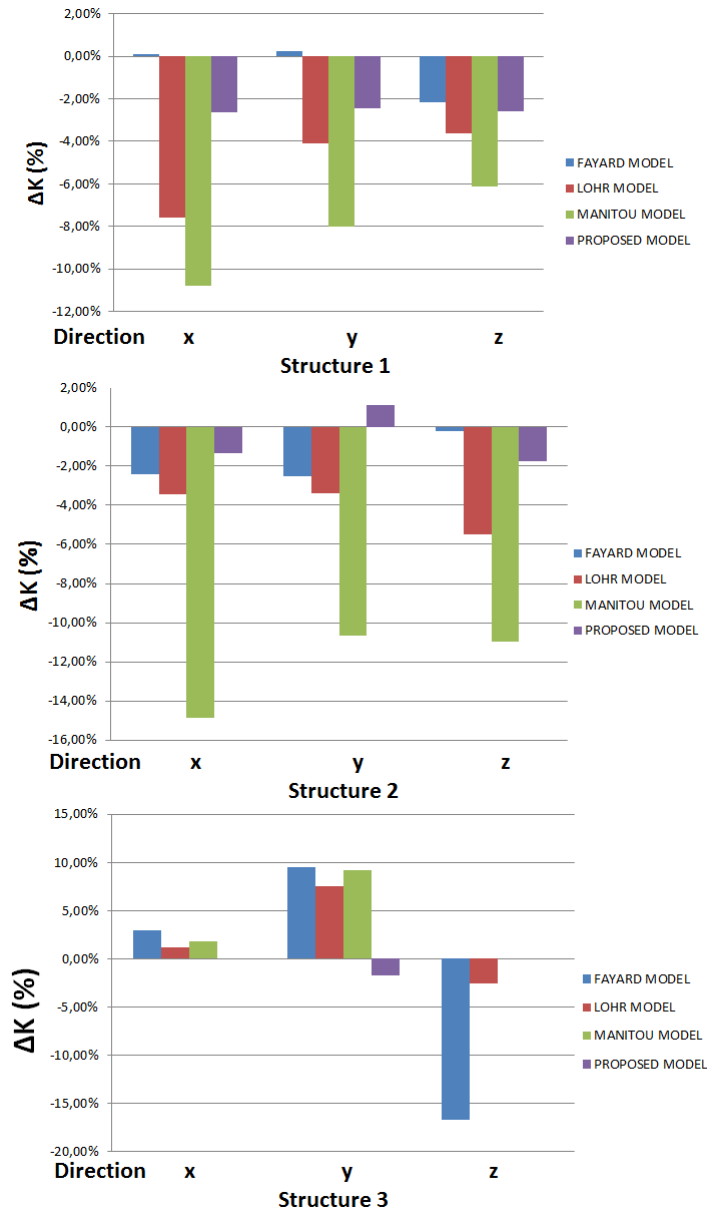


Fig. 9. Stiffness comparison results for the Manitou, Fayard, Lohr models and the proposed approach with reference to a full-solid element model on welded structures 1,2,3

Good correlation between the proposed model and the reference model is observed for the 3 welded structures. The maximum difference is 2,7% for structure 1, loaded in the \bar{y} direction. These results are consistent with the Fayard model and the Lohr model. However, the results from the model currently used by Manitou show a maximum difference greater than 10% for 4 of the configurations studied. The differences between the 4 models can be explained by the level of complexity used to model the welded assemblies. The local stiffness of the weld is not considered in the model currently used by Manitou, and it is idealized by specific meshing rules in the Fayard and the Lohr models. In the proposed approach the local geometry of the weld is fully considered at the expense of greater calculation time. However it should be noted that this is mainly pre-processing necessary to establish a library of weld geometries. The proposed model seems to be a good alternative to the current ones, however, other welded assemblies should be tested in order to confirm these initial results.

5. Conclusion

This work focuses on the fatigue design of welded assemblies. For this, a numerical strategy to consider the impact of the welds on the overall stiffness of these assemblies has been proposed. The proposed method to model welded structures is based on a combined surfacic-volumetric approach. Weld areas are modelled using solid elements in order to take into account the real stiffness of the weld while steel sheets are modelled using shell elements. In order to limit computational costs, the local models of the welds are condensed into an equivalent stiffness matrix and then, the equivalent stiffness matrix is inserted into the global shell elements model. After calculation, from displacements at the connecting nodes of the stiffness equivalent matrix, the local stress state at weld toes and weld root can be determined. To validate the stiffness behaviour of this method, three elementary welded assemblies have been modelled using solid elements as the reference case and two other methods from the literature. The results show good correlation between the proposed approach and the reference models for three different structures. These comparisons highlight the improvement that can be easily achieved in terms of the model currently used by Manitou.

Future work will focus on the fatigue evaluation of welded assemblies, textcolorblueonce the weld stiffness and consequently the local stresses are accurately known. Fatigue tests on 4 elementary welded structures are being carried out to estimate the influence of the stress gradient at the hot spot as well as size effects. Then, from an analysis of the experimental data and by knowing the local stress state at the hot spots, an equivalent stress will be defined in order to obtain a single 'master' Wöhler curve taking into account the stress gradient, the size effect and the stress multiaxiality. The validation process of the method will include a fatigue test on a full scale chassis structure.

References

- [1] Bennebach, Dimensionnement des assemblages soudés en fatigue. état de l'art sur les méthodes et techniques de modélisations éléments finis. confrontations de certaines approches à des résultats d'essais, Cetim, N/Réf : 2018/4S/AC/MBEN /CTHII (2018).
- [2] Osawa, Sawamura, Shota, Suzuki, Study on the relationship between shell and solid stresses in the vicinities of web stiffened cruciform joints, IIW, XIII-2288-09 (2009).
- [3] Hoff, Mueller, Wallerstein, Weld modeling with msc.nastran (2000).
- [4] Fricke, Iiw guideline for the assessment of weld root fatigue, IIW-Doc. XIII-2380r1-11/XV-1383r1-11 57 (2013) 753–791.
- [5] Fayard, Dimensionnement à la fatigue polycyclique de structures soudées, Ph.D. thesis, Palaiseau, Ecole polytechnique (1996).
- [6] Turlier, Klein, De Noni, Lawrjaniec, Fea shell element model for enhanced structural stress analysis of seam welds, Procedia Engineering (2011).
- [7] Dang Van, Bignonnet, Fayard, Janosch, Assessment of welded structures by a local multiaxial fatigue approach 24 (2001) 369 – 376.
- [8] Fermér, Andréasson, Frodin, Fatigue life prediction of mag-welded thin-sheet structures, SAE International (1998).
- [9] Klein, Turlier, Ober, Fea structural stress of modalohr system for semi-trailer rail transportation: Weld root fatigue focus, Procedia Engineering 66 (2013) 79 – 87.
- [10] Fezans, Analyse linéaire et non linéaire géométrique des coques par éléments finis isoparamétriques tridimensionnels dégénérés, Theses, École Nationale Supérieure de l'Aéronautique et de l'Espace de Toulouse (1981).